Heliyon 10 (2024) e33933

Contents lists available at ScienceDirect

Heliyon

journal homepage: www.cell.com/heliyon

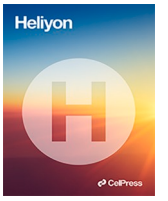

Research article

EV-miRNAs from breast cancer patients of plasma as potential prognostic biomarkers of disease recurrence

Rhafaela Lima Causin [a,1], Mariana Regatieri Polezi [a,1], Ana Julia Aguiar de Freitas [a,1], Stéphanie Calfa [a], Wanessa Fernanda Altei [a,b], Júlia Oliveira Dias [a], Ana Carolina Laus [a], Danielle Pessôa-Pereira [a], Tatiana Takahasi Komoto [a], Adriane Feijó Evangelista [a,c], Cristiano de Pádua Souza [d], Rui Manuel Reis [a,e,f], Marcia Maria Chiquitelli Marques [a,*]

[a] *Molecular Oncology Research Center, Barretos Cancer Hospital, Barretos, São Paulo, 14784-400, Brazil*
[b] *Radiation Oncology Department, Barretos Cancer Hospital, Barretos, São Paulo, 14784-400, Brazil*
[c] *Sergio Arouca National School of Public Health, Oswaldo Cruz Foundation, Manguinhos, Rio de Janeiro, 21040-361, Brazil*
[d] *Barretos Cancer Hospital, Barretos, São Paulo, 14784-400, Brazil*
[e] *Life and Health Sciences Research Institute (ICVS), Medical School, University of Minho, Braga, 4710-057, Portugal*
[f] *ICVS/3B's-PT Government Associate Laboratory, Braga, 4710-057, Portugal*

ARTICLE INFO

Keywords:
Breast cancer
Extracellular vesicles
MicroRNA
Biomarkers
Disease recurrence

ABSTRACT

Background: Extracellular vesicles (EVs), ubiquitously released by blood cells, facilitate intercellular communication. In cancer, tumor-derived EVs profoundly affect the microenvironment, promoting tumor progression and raising the risk of recurrence. These EVs contain miRNAs (EV-miRNAs), promising cancer biomarkers. Characterizing plasma EVs and identifying EV-miRNAs associated with breast cancer recurrence are crucial aspects of cancer research since they allow us to discover new biomarkers that are effective for understanding tumor biology and for being used for early detection, disease monitoring, or approaches to personalized medicine. This study aimed to characterize plasma EVs in breast cancer (BC) patients and identify EV-miRNAs associated with BC recurrence.

Methods: This retrospective observational study included 24 BC patients divided into recurrence (n= 11) and non-recurrence (n= 13) groups. Plasma EVs were isolated and characterized. Total RNA from EVs was analyzed for miRNA expression using NanoString's nCounter® miRNA Expression Assays panel. MicroRNA target prediction used mirDIP, and pathway interactions were assessed via Reactome.

Results: A stronger presence of circulating EVs was found to be linked with a less favorable prognosis ($p = 0.0062$). We discovered a distinct signature of EV-miRNAs, notably including miR-19a-3p and miR-130b-3p, which are significantly associated with breast cancer recurrence.

* Corresponding author.
E-mail addresses: rhafaela-lima@hotmail.com (R.L. Causin), marianapolezi@hotmail.com (M.R. Polezi), aaguiardefreitas@gmail.com (A.J.A. Freitas), stephaniecalfa@outlook.com (S. Calfa), wanaltei@gmail.com (W.F. Altei), julia.odias@yahoo.com.br (J.O. Dias), anacarolinalaus@gmail.com (A.C. Laus), dpessoapereira@uiowa.edu (D. Pessôa-Pereira), tattytk@hotmail.com (T.T. Komoto), adriane.feijo@gmail.com (A.F. Evangelista), crispadua10@gmail.com (C.P. Souza), ruireis.hcb@gmail.com (R.M. Reis), mmcmsilveira@gmail.com (M.M.C. Marques).
[1] These authors have contributed equally to this study.

https://doi.org/10.1016/j.heliyon.2024.e33933
Received 20 October 2023; Received in revised form 28 June 2024; Accepted 1 July 2024
Available online 10 July 2024

Furthermore, miR-19a-3p and miR-130b-3p were implicated in the regulation of PTEN and MDM4, potentially contributing to breast cancer progression.
A notable association emerged, indicating a high concentration of circulating EVs predicts poor prognosis ($p = 0.0062$). Our study found a distinct EV-miRNA signature involving miR-19a-3p and miR-130b-3p, strongly associated with disease recurrence. We also presented compelling evidence for their regulatory roles in PTEN and MDM4 genes, contributing to BC development.
Conclusion: This study revealed that increased plasma EV concentration is associated with BC recurrence. The prognostic significance of EVs is closely tied to the unique expression profiles of miR-19a-3p and miR-130b-3p. These findings underscore the potential of EV-associated miRNAs as valuable indicators for BC recurrence, opening new avenues for diagnosis and treatment exploration.

Abbreviations

BC	Breast cancer
ER	Estrogen receptor
EV	Extracellular vesicles
EV-miRNAs	EV-derived miRNAs
FC	Fold-change
FDR	False Discovery Rate.
HER2	Human epidermal growth factor receptor 2
METABRIC	Molecular Taxonomy of Breast Cancer International Consortium
miRNAs	MicroRNAs
mRNA	Messenger RNA
NTA	Nanoparticle tracking analysis
OS	Overalll survival
PR	Progesterone receptor
RFS	Relapse-free survival
RNAseq	RNA sequencing
TCGA	The Cancer Genome Atlas Program

1. Introduction

Breast cancer (BC) is the most commonly diagnosed and frequent cancer type in women worldwide, accounting for 25% of all cancers and the leading cause of cancer-related deaths among women [1,2]. It is a highly heterogeneous disease that can be characterized by varying expression levels of the estrogen receptor (ER), progesterone receptor (PR), and human epidermal growth factor receptor 2 (HER2). Clinically, these markers have become crucial in defining breast cancer, providing valuable information for prognosis and guiding treatment approaches [3,4]. These distinct profiles directly influence tumor behavior, including recurrence, drug resistance, mortality rate, and therapeutic approaches. Nevertheless, these markers do not fully capture disease behavior and additional clinical biomarkers are warranted [5–7]. Therefore, extracellular vesicles (EVs) have emerged as potential biomarkers for diagnosis, prognosis, and prediction therapy using liquid biopsy [8].

EVs are secreted by various cells and can encapsulate a range of biomolecules reflective of their cell of origin, including microRNAs (miRNAs or miRs), known as EV-derived miRNAs (EV-miRNAs) [9]. These small vesicles are released by cells into the extracellular environment and are surrounded by a lipid bilayer. They contain proteins and nucleic acids, exhibiting high heterogeneity and various classifications [10]. EVs are classified based on their diameter (small extracellular vesicles (sEVs) < 200 nm; medium/large EVs (m/lEVs) > 200 nm) and density (low, medium, high), but the classification can also vary according to specific markers or origin [11]. EVs are involved in cell-to-cell communication and could also be involved in tumor development [12]. Noteworthy, it has been demonstrated that these vesicles are associated with diagnosis, disease recurrence, and chemoresistance in many types of cancers, mainly because EVs can carry small molecules, such as miRNAs, to distant sites, contributing to the formation of pre-metastatic sites [13].

miRNAs are a broad class of endogenous, single-stranded, non-coding small RNAs from 19 to 25 nucleotides in length. Their primary role is the post-translational regulation of genes involved in numerous biological processes, included proliferation, apoptosis, tumorigenesis, cellular differentiation, metastasis, and chemoresistance [14,15]. Therefore, miRNAs are linked to a variety of biological functions and can be utilized for disease treatment and diagnosis, as biomarkers, or as new therapeutic targets [16–19]. In addition, these small molecules and their ability to function without complete base pairing enable a single miRNA to regulate multiple mRNA targets, while several miRNAs can work together to control a single mRNA within a critical gene expression regulatory network [20,21].

Using EV-miRNAs from liquid biopsy has shown promising results in identifying potential biomarkers [22]. A study compared EV-miRNA profiles between BC patients with and without relapse disease. The authors found a panel of differentially expressed EV-miRNAs in the serum of those patients, suggesting that these EV-miRNAs could be used to monitor the disease [23].

The aim of this study was to assess the prognostic role of EV-miRNAs isolated from BC patients' plasma. This study analyzed patients who had either presented or had not presented disease recurrence after treatment and in follow-up for more than 60 months.

Using a robust platform, we assessed the expression profile of 800 miRNAS, and found 32 miRNAs differentially expressed between patients with BC recurrence and those without BC recurrence. Following this, we identified that miR-19a-3p and miR-130b-3p were accurate and associated with BC in recurrence status compared to other miRNAs, suggesting that these miRNAs could be valuable recurrence biomarkers. Finally, *in silico* analysis identified *MDM4* and *PTEN* as potential targets of EV-miR-19a-3p and EV-miR-130b-3p, leading to alteration of the p53 pathway in BC.

2. Materials and methods

2.1. Study design

This retrospective observational study included 24 women (aged ≥18 years), diagnosed with breast cancer, stage I–III, never-treated, who have not submitted prior surgery or systemic therapy and who have availability of plasma at the Barretos Cancer Hospital Biobank [24]. Cases with a follow-up of less than 60 months or insufficient material for analysis (plasma) were excluded from this study. All patients signed an informed consent. The patients were divided into two groups: Group 1 represents the cases with BC recurrence (n= 11), and Group 2, cases without recurrence disease (n= 13).

Other parameters, such as clinical-pathological characteristics, treatment type, and metastasis information, were also analyzed. All data were managed on the REDCap platform [25].

2.2. Extracellular vesicles isolation from plasma samples and RNA isolation

EVs were isolated from plasma samples by ultracentrifugation (Thermo Fisher Scientific, Inc. Sorvall WX + Ultracentrifuge Series; TH-660 Swinging Bucket Rotor) following the manufacturer's instructions and available literature. In summary, 1 mL of each plasma sample was used, and three protease inhibitors were added: 1.5 μL of aprotinin, 1.5 μL of leupeptin, and 15 μL of PMSF (all reagents were purchased from Sigma-Aldrich). In order to reduce possible fibrin residues, the homogenized product was centrifuged for 1 min (7600 rpm) at room temperature using the AG 5424 Microcentrifuges (Eppendorf, Hamburg, Germany). The forming pellet was discarded. Then the supernatant was transferred to another tube with 1 mL of Dulbecco's phosphate-buffered saline (DPBS, Thermo Fisher Scientific, Inc.) until complete homogenization, followed by adding more 4 mL as per the manufacturer's instructions. The samples were submitted to two ultracentrifugations at 140.000×*g* at 4 °C, the first one for 150 min, all supernatants were discarded, and the homogenization process was repeated as stated above. After that, the second centrifugation occurred for 90 min. Following, the supernatant was discarded, and the pellet was resuspended in 420 μL of DPBS. From this solution, 10 μL was used for quantification by NanoSight, and 300 μL was used for miRNA extraction and western blotting.

The RNA isolation was performed by miRNeasy Mini Kit (Catalog number 217084, Qiagen, Germany) according to the manufacturer's protocol, and the total RNA was evaluated by NanoDrop Spectrophotometer v3.7 (Thermo Fisher Scientific, Inc.).

2.3. Nanoparticle tracking analysis (NTA)

EVs were quantified using nanoparticle tracking analysis (NTA) using the NanoSight NS300 (Malvern Panalytical, Malvern, United Kingdom) platform according to the manufacturer's protocol, software NTA 3.2 version (NanoSight Ltd, Amesbury, United Kingdom). This platform contains a supersensitive optical laser and detects particles' Brownian movements. Using the Stokes-Einstein equation, determines the diameter, concentration, and distribution of the particles. This method is considered the gold standard for the quantification and size analysis of nanoparticles. EV samples were diluted in 999 μL of ultrapure water to 1 μL of EVs isolated from plasma, and analyzed by 4 times 60-s captures, with the following parameters: screen gain: 2.0, camera level: 14, blur: auto, max jump distance: 14.6, min track length: auto.

2.4. Cell culture and whole cell lysate

Triple-negative breast cancer cells (MDA-MB-231) were cultivated in Dulbecco's Modified Eagle Medium (DMEM) supplemented with fetal bovine plasma (10% FBS) and sodium pyruvate (1% SP) at 37° C, 5% CO_2. After three subcultures, cells were cultivated in 6-well plates (5×10^5 cells/well) at 37° C, 5% CO_2 overnight. On the ice, cells were washed with PBS, then 60 μL of lysis buffer (50 mM Tris-HCl, pH 7.4; 1% tween-20, 0,25% deoxycholate, 150 mM NaCl, 1 mM EDTA, 1 mM sodium orthovanadate, 1 mM sodium fluoride, 0.1 mM PMSF, 1 μg/mL aprotinin, 1 μg/mL leupeptin and 1 μg/mL DTT) were added to each well and the cell lysate was collected using a cell scraper. Samples were kept on ice for 1 h and then centrifuged at 13.000 rpm for 15 min at 4° C. The supernatant was collected and used for protein quantification.

2.5. Protein quantification

MDA-MB-231 cell lysates and isolated EV samples were quantified using a microBCA kit (Thermo Fisher Scientific, Inc.), according to the manufacturer's instructions.

2.6. Western blotting

For protein separation by electrophoresis, 5 μg of each sample were boiled for 5 min at 95° C, put on ice, mixed with Laemmli sample buffer, and applied to 10% SDS-PAGE gels with Precision Plus Dual Color (Bio-Rad) as loading control for 100 min at 90 V.

Following separation, proteins were transferred to nitrocellulose membranes (0.45 μm, Amersham Biosciences) by semi-dry transfer (Amersham Biosciences) for 4 h. Membranes were then stained with Ponceau S dye, washed with deionized water, photographed, and washed with TBS-T buffer (30 g of Tris, 80 g of NaCl, pH 7.6, 0,1% Tween 20).

The primary antibodies used as probes are presented in Supplementary Table S1. All primary antibodies were diluted at 1:1000, probed after blocking the membrane with blocking buffer (3% BSA in TBS-T buffer) for 1 h, and kept at 4° C overnight on a shaker. The appropriate secondary antibodies were diluted in 5% non-fat milk and incubated for 1 h at room temperature on a shaker: IgG Goat anti-Mouse HRP (1:10.000, ab205719, Abcam) and IgG Goat anti-Rabbit HRP (1:10.000, ab205718, Abcam). Between incubations, membranes were stripped with Restore Western Blot Stripping Buffer (Thermo Fisher Scientific, Inc.), washed, and blocked with blocking buffer for 1 h.

Membranes were revealed with 90% of ECL substrate (32209, Thermo Fisher Scientific, Inc.) and 10% of SuperSignal West Femto (34094 Thermo Fisher Scientific, Inc.) for 2 min, scanned on an ImageQuant LAS 4000 mini-imaging system (GE Healthcare Life Sciences) and analyzed using FIJI ImageJ and Bio-Rad ImageLab.

2.7. EV-miRNAs expression assay from plasma

The miRNA expression profile of 24 cases was assessed using the nCounter® miRNA Expression Assays panel (NanoString Technologies, Seattle, WA, USA), as previously reported [26,27]. However, a sample referring to group 1 (disease recurrence) had to be excluded because it was outside the quality standards, making a total of twenty-three samples, ten representing the cases with BC recurrence and thirteen the cases without recurrence disease. This panel consists of 800 targets for different cancer-associated miRNAs (http://www.nanostring.com/products/miRNA) and allows the expression analysis of different miRNAs in different types and subtypes of tumors. 50 ng of total RNA underwent to sample preparation which involved the ligation of specific tags on miRNAs, followed by purification and hybridization with Capture and Reporter CodeSet probes (nCounter Human v3 miRNA Expression Assay), according to manufacturer's instructions (NanoString Technologies, Seattle, WA, USA). RNA-probes complexes were purified and immobilized on cartridges using PrepStation System (NanoString Technologies, Seattle, WA, USA), followed by data acquisition on Digital Analyzer Station (NanoString Technologies, Seattle, WA, USA), capturing 555 fields of view (FOV). Experimental quality controls parameters, such as Ligation Control, Limit of Detection, and Binding Density, were initially evaluated by nSolver Software (NanoString Technologies, Seattle, WA, USA). One sample was excluded from the analysis of miRNA expression due to quality control issues.

2.8. miRNA target prediction in silico

MicroRNA targets prediction was performed using miRDIP (microRNA Data Integration Portal (https://ophid.utoronto.ca/mirDIP/) [28], a tool that integrates 30 databases (BCmicrO, BiTargeting, CoMeTa, Cupid, DIANA, ElMMo3, GenMir ++, MAMI, MBStar, microrna.org, MirAncesTar, mirbase, miRcode, mirCoX, miRDB, MirMAP, MirSNP, MirTar, miRTar2GO, Mirza-G, MultiMiTar, PACCMIT, PicTar, PITA, RepTar, RNA22, RNAhybrid, TargetRank, Targetscan, TargetSpy) comprising almost 152 million predictions of human miRNA-mRNA. These databases consider individual characteristics for miRNA target prediction, such as: pairing with the seed sequence, conservation, free binding energy, accessibility to the binding site, multiple binding sites, ALU sequence content, and sequence adjacent to the mRNA. Then, it attributes an integrative score to each unique target miRNA interaction, statistically inferred. Unidirectional analysis was performed in the miRDIP tool [28,29], in which we considered the miRNAs that reached the AUC $\geq$0.70 and considered the minimum Very High-quality score (Top 1%), and targets predicted into 30 algorithms were used in miRDIP analysis.

2.9. Enrichment of biological pathways

Biological pathway enrichment was analyzed using the Reactome plugin in Cytoscape software v.3.9.1 (Seattle, WA, USA, https://cytoscape.org/), which provides regulatory interactions and pathways from Reactome databases. For the analysis, only genes associated with breast carcinoma, as identified by the Cancer Gene Index Annotations (provided by the National Cancer Institute, NCI), were selected using the Load Cancer Index function available in ReactomeFIViz. Pathways were considered significant if they had FDR values $\leq$ 0.001 and included at least three genes.

2.10. GEPIA 2 analysis

The GEPIA 2 database (http://gepia2.cancer-pku.cn/#analysis) was used to examine*MDM4* and *TP53* expression in BC tissues (classified as BRCA at GEPIA 2) [30]. The breast cancer dataset was selected, and *PTEN, MDM4*, and *TP53* levels in BRCA (n = 1082) and non-tumor tissues (n = 291) were plotted.

2.11. In silico evaluation of relapse-free survival and overall survival

To calculate the relapse-free survival (RFS) and overall survival (OS) *in silico* we used the online tool at Kaplan-Meier plotter https://kmplot.com/, which is a validation of survival biomarkers and capable of assessing the effect of 54 k genes (mRNA, miRNA, and protein) on survival in 21 cancer types. A total of 1262 BC patients from the (Molecular Taxonomy of Breast Cancer International Consortium) database and 1880 BC patients from The Cancer Genome Atlas Program (TCGA) database had complete follow-up data, pathological information, and genes and miRNAs expression levels. All the details concerning how to use online web tools have been described in the paper published by Lanczky et al. [31]. We used RNA sequencing data (RNAseq) from TCGA database using the Affymetrix platform ID 225363_at, 225740_x_at and 201746_at_x_at datasets, to evaluate the OS and RFS for the *PTEN*, *MDM4* and *TP53* Genes, respectively. To evaluate *in silico* the OS for the miRNAs, miR-19a-3p and miR-130b-3p, we used the METABRIC dataset. The difference between the date of diagnosis and the date of the event (recurrence and/or death) were used to calculate RFS and OS, respectively.

2.12. Statistical and bioinformatics analysis

We collected and pre-processed the raw data using nSolver™ Analysis Software v4.0 (NanoString Technologies). Subsequently, data normalization was conducted in the R statistical environment (R-project 4.3.1; The R Foundation, Viena, Austria) using the NanoStringNorm package from Bioconductor. miRNAs counts were normalized employing a method based on the lowest coefficient of variation (low CV). Differential expression analysis was performed using the limma package from Bioconductor within the R environment. Normalized data were log2-transformed and utilized for differential expression analysis, assuming a significance level of $p < 0.05$ and fold-change> 1.5 between the evaluated groups. Heatmaps were made from differential expression data of miRNAs using the Complex Heatmap package. Next, we performed the area under the curve (AUC) of the ROC. We calculated the sensitivity and

Table 1
Patient's clinical pathological characteristics and *BC* recurrence status.

Characteristics		Total		BC recurrence				p-value
		(n = 24)		Yes (n = 11)		No (n = 13)		
		n (sd, %)		n	(sd, %)	n	(sd, %)	
Age (years)	Mean (sd)	46	(sd = 8)	44	(sd = 7)	48	(sd = 8)	0.244
	min-max	31–62		34–52		31–62		
BMI	Mean (sd)	27	(sd = 7)	27	(sd = 7)	27	(sd = 7)	0.685
	min-max	18–47		18–41		22–27		
FHC	No	10	(41.7)	4	(36.4)	6	(46.2)	0.628
	Yes	14	(58.3)	7	(63.6)	7	(53.8)	
HT	Never-user	3	(12.5)	3	(27.3)	–	-	0.127
	Tamoxifen	15	(62.5)	6	(54.5)	9	(69.2)	
	Anastrozole	6	(25.0)	2	(18.2)	4	(30.8)	
ER	Positive	21	(87.5)	8	(72.7)	13	(84.6)	*0.044*
	Negative	3	(12.5)	3	(27.3)	0	(15.4)	
PR	Positive	19	(79.2)	8	(72.7)	0	(87.9)	0.475
	Negative	5	(20.8)	3	(27.3)	13	(100.0)	
HER2+	Positive	7	(29.2)	4	(36.4)	3	(23.1)	0.476
	Negative	17	(70.8)	7	(63.6)	10	(76.9)	
Histological Grade	G1	2	(8.3)	1	(9.1)	1	(7.7)	0.250
	G2	9	(37.5)	6	(54.5)	3	(23.2)	
	G3	13	(54.2)	4	(36.4)	9	(69.2)	
Surgery	Quadrantectomy	13	(54.2)	4	(36.4)	9	(69.9)	0.107
	Mastectomy	11	(45.8)	7	(63.6)	4	(30.8)	
CT	No	3	(12.5)	2	(18.2)	1	(7.7)	0.051
	NAC	7	(29.2)	4	(36.4)	3	(23.1)	
	AC	11	(45.8)	2	(18.2)	9	(69.2)	
	NAC + AC	3	(12.5)	3	(27.3)	-	-	
Relapse	Bones	5	(50.0)	5	(50.0)	–	–	*<0.001*
	2 or more sites	4	(40.0)	4	(40.0)	–	–	
	Others	1	(10.0)	1	(10.0)	–	–	
Metastasis	No	9	(37.5)	9	(81.8)	13	(100)	*<0.001*
	Yes	15	(62.5)	2	(18.2)	–	–	
Survival status	AWD	14	(60.9)	1	(10.0)	13	(100)	*<0.001*
	AWI	1	(4.3)	1	(10.0)	–	–	
	NCRD	1	(4.3)	1	(10.0)	–	–	
	CRD	7	(30.4)	7	(70.0)	–	–	

Chi-square test or ANOVA test of the association of clinicopathological features in breast cancer with recurrence status (yes or no). BC: breast cancer; BMI: Body mass index; FHC: Family history of cancer; HT: hormone therapy; ER: estrogen receptor; PR: progesterone receptor; CT: chemotherapy; NAC: neoadjuvant chemotherapy; AC: adjuvant chemotherapy; AWD: alive without disease; AWI: alive with illness; NCRD: non-cancer related death; CRD: cancer-related death. p-value <0.05 is significant.

specificity to determine the accuracy of the differentially expressed miRNAs using ggplot2, PROC, and ROCR package from Bioconductor.

The clinical-pathological features were characterized using descriptive statistics between two groups (BC patients with and without disease recurrence), using the Chi-square test or ANOVA test. Overall patient survival (OS), defined as the time from diagnosis until death or clinical and/or radiologic disease recurrence, was the primary endpoint in patients who presented disease recurrence.

All statistical analyses of the data obtained from the NTA, and the western blotting were performed on GraphPad Prism (v. 9.0.0). The data sets were submitted to Shapiro-Wilk normality tests. Next, we used a non-parametric test and analyzed all the data by the Mann-Whitney test. Values of $p < 0.05$ were considered statistically significant. Results were presented as median expression ± interquartile range.

A total of 2976 patients were included in the analysis GEPIA. patients were stratified into high- and low-expression groups based on the median expression of both genes. Survival analysis was conducted using Kaplan-Meier curves, and the two groups were compared using a log-rank test.

3. Results

3.1. Study population and prognostic factors associated with disease recurrence

The main clinical pathological characteristics of the 24 patients with BC are summarized in Table 1. The median age was 46 years old (range 31–62 years, SD= 8 years). In a univariate analysis, we identified estrogen receptor status (ER, p= 0.044), BC recurrence ($p < 0.001$), metastasis ($p< 0.001$), and survival status ($p < 0.001$) showed significant differences when comparing groups.

3.2. Characterization of EVs isolated from BC patient's plasma

Purified plasma EVs were characterized by Western blotting and particle size analysis. On the western blotting analysis, we evaluated the presence of classic EV markers (CD63, ALIX, and Flotillin-1) and negative control (Calnexin) (Fig. S1). All EV markers were observed in both groups, while the negative control was detected only in the MDA-MB-231 whole cell lysate (Fig. 1A–C). The concentration of EV markers had no significant differences between the two groups. Nanoparticle analysis showed that most EVs had

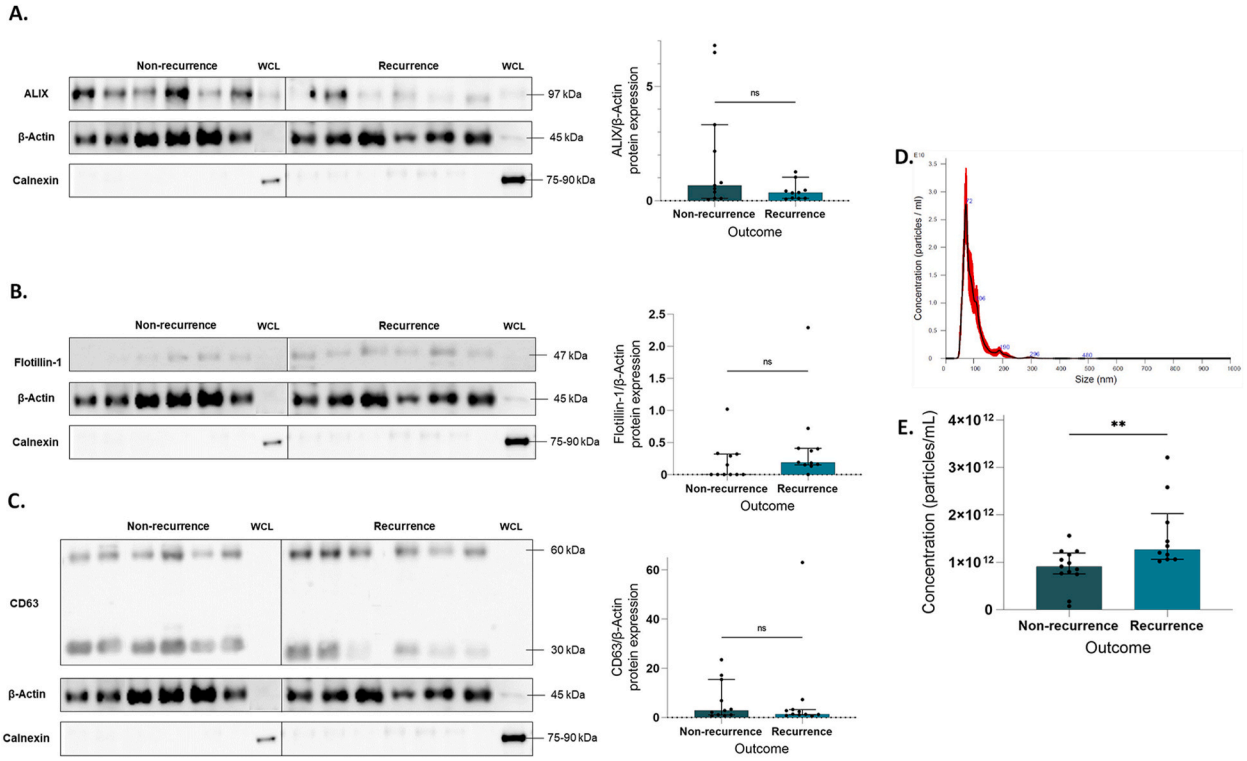

Fig. 1. Characterization of the EVs isolated from breast cancer patients' plasma. A-C. Western blot analysis for three EV markers (ALIX, Flotillin-1, and CD63), positive control (β-Actin), and negative control (Calnexin) (median ± interquartile). D. Nanoparticle tracking analysis results showed the relative concentration of isolated particles (particles/mL) and their size mostly at 72 nm. The images demonstrate six representative samples from each group. However, western blotting was performed for all 24 samples (group 1, n= 11 and group 2, n= 13). E. Dot plots representing EVs mean concentration in the plasma samples (**p= 0.0062). ns = not statistically significant; WCL: whole cell lysate.

an average size of 72 nm, consistent with the size range of typical small EVs (Fig. 1D).

When comparing the concentration of circulating EVs among groups, we observed that patients with BC recurrence had a significantly higher concentration of EVs than the group without recurrence (p= 0.0062, Fig. 1E).

3.3. EV-miRNAs expression signature from plasma

We then performed miRNA expression profiling using the nCounter Human v3 miRNA Expression panel to identify differentially expressed miRNAs (*t*-test ($p < 0.05$), fold change ≥1.5) among both BC groups. In the graphical representation demonstrated by the unsupervised hierarchical analysis heatmap of miRNAs (Fig. 2), we can see thirty-four miRNAs with significant differences when comparing groups ($p < 0.05$). Of these thirty-four miRNAs, thirty-two presents fold change ≥1.5, eleven had a low expression, while twenty-one of them presented a high-expression (Table 2).

3.4. miRNAs and predicted targets in molecular pathways of BC and in silico validation

Considering the 32 differentially expressed miRNAs, two of them (miR-19a-3p and miR-130b-3p) were previously associated with genes described for breast tumors according to the Cancer Gene Index Annotations (provided by the National Cancer Institute, NCI) [32]. In this context, we identified genes potentially predicted that could be targets of these miRNAs. Then, a target miRNA-RNAm interaction network was assessed on Cytoscape [33], from which we can observe the interaction networks between the miRNA and its predicted target genes.

Of the miRNA-RNAm interaction network, we found the *PTEN* and *MDM4* genes regulated by miR-19a-3p and miR-130b-3p that have previously been implicated in BC-related pathways (Table 3 and Fig. 3A). Furthermore, through *in silico* functional enrichment analysis of key biological pathways involved in breast carcinogenesis, we identified *PTEN* and *MDM4* as the most significantly associated genes with breast cancer (Table 3, Fig. 3A). Notably, both miRNAs, miR-19a-3p and miR-130b-3p, were predicted to target and potentially regulate the expression of PTEN and MDM4. Accordingly, we found that *PTEN* and *MDM4* were related to pathways, microRNAs in cancer, and the p53 signaling pathway (Table 3 and Fig. 3B).

Since the p53 signaling pathway was enriched and potentially regulated by miR-19a-3p and miR-130b-3p, we further evaluated the *in silico* expression of *TP53*, as well as the *PTEN,* and *MDM4* genes. The *PTEN*, *MDM4* and *TP53* gene expression levels, were compared between breast cancer and adjacent non-tumor tissues from patients using original published data in the GEPIA database. The results

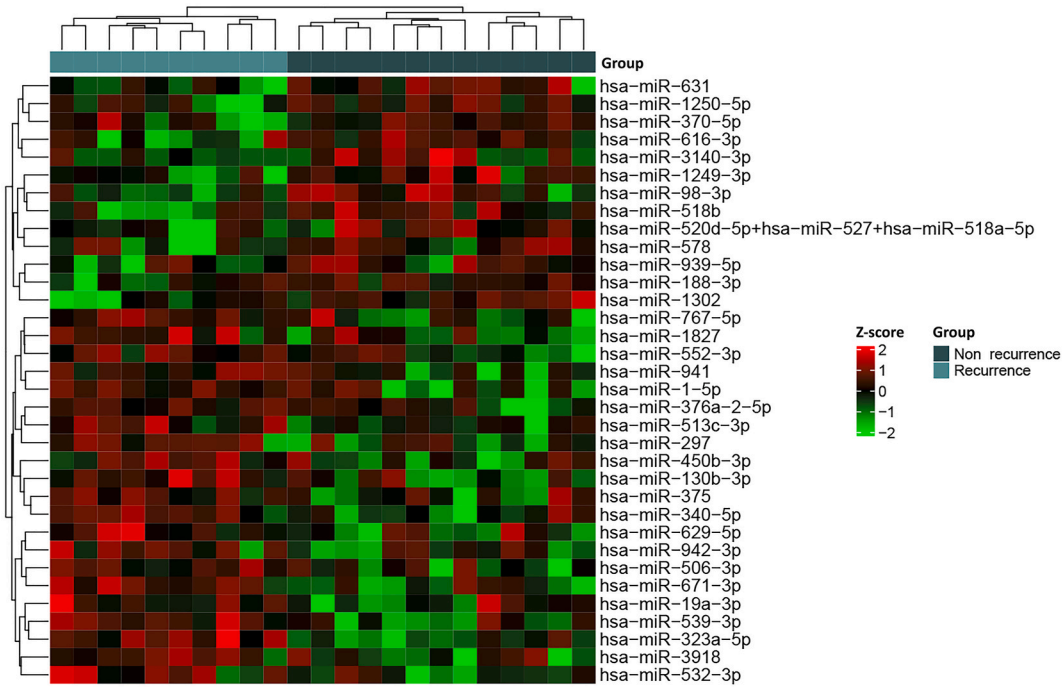

Fig. 2. The heatmap of unsupervised hierarchical analysis of the 34 miRNAs differentially expressed by nCounter miRNA expression technology. Student's T test was used to compare the miRNA expression differences between the two study groups: patients with disease recurrence (light green bar, n= 10) and patients without disease recurrence (dark green bar, n= 13). Thirty-four miRNAs displayed statistically significant results ($p < 0.05$). Samples are arranged in columns, miRNA expression levels are in rows, and both are hierarchically clustered using Euclidean distance with the average linkage of nodes. Red shades indicate increased relative expression; green shades indicate reduced expression; black indicates median expression. (For interpretation of the references to color in this figure legend, the reader is referred to the Web version of this article.)

Table 2
Summarizing the 32 differentially expressed miRNAs data according to BC recurrence status.

miRNAs	Fold change	P-value
miR-518b	−2.70	<0.001
miR-98–3p	−2.23	0.0013
miR-578	−2.19	0.0019
miR-1250–5p	−2.18	0.0023
miR-616–3p	−1.99	0.0047
miR-520 d-5p + miR-527+miR-518a-5p	−1.94	0.0086
miR-631	−1.86	0.0092
miR-188–3p	−1.85	0.0103
miR-370–5p	−1.81	0.0115
miR-1302	−1.79	0.0134
miR-3140–3p	−1.76	0.0137
miR-532–3p	1.50	0.0196
miR-340–5p	1.57	0.0205
miR-767–5p	1.59	0.0207
miR-629–5p	1.62	0.0210
miR-1827	1.64	0.0253
miR-450b-3p	1.67	0.0256
miR-552–3p	1.75	0.0259
miR-539–3p	1.81	0.0266
miR-375	1.85	0.0314
miR-130b-3p	1.86	0.0316
miR-1-5p	1.87	0.0327
miR-513c-3p	1.96	0.0329
miR-376a-2-5p	1.96	0.0374
miR-941	1.98	0.0409
miR-506–3p	2.04	0.0451
miR-19a-3p	2.10	0.0454
miR-942–3p	2.11	0.0461
miR-671–3p	2.21	0.0462
miR-3918	2.23	0.0478
miR-297	2.27	0.0486
miR-323a-5p	2.36	0.0499

Student's T test was used to compare the miRNA expression differences between the two study groups: patients with disease recurrence (n= 10) and patients without disease recurrence (n= 13). Thirty-two miRNAs displayed statistically significant results ($p < 0.05$) and fold-change ≥ 1.5.

Table 3
Pathway enrichment analysis for miR-19a-3p and miR-130b-3p and genes associated with breast cancer.

Pathways	E-score	P-value	FDR	Genes
MicroRNAs in cancer(K)	0.0261	<0.001	<0.001	*BMPR2,* ***PTEN****, RPS6KA5, SOX4, ZEB2, PIK3CA, MET, THBS1,* ***MDM4***
Pathways in cancer(K)	0.0447	<0.001	<0.001	***PTEN****, RPS6KA5, NCOA1, TGFBR2, PIK3CA, PPARG, PLCB1, MET, TCF7L2, IGF1, ESR1*
Breast cancer(K)	0.0124	<0.001	<0.001	***PTEN****, NCOA1, PIK3CA, TCF7L2, IGF1, ESR1*
Signaling events mediated by focal adhesion kinase(N)	0.0051	<0.001	<0.001	*WASL, PIK3CA, RAP1B, RAP1A*
MTOR signaling pathway(B)	0.0020	<0.001	<0.001	***PTEN****, TSC1, PIK3CA*
Adherens junction(K)	0.0060	<0.001	<0.001	*WASL, TGFBR2, MET, TCF7L2*
Proteoglycans in cancer(K)	0.0173	<0.001	<0.001	*PIK3CA, MET, THBS1, IGF1, ESR1, SDC1*
p53 signaling pathway(K)	0.0061	<0.001	<0.001	***PTEN****, THBS1, IGF1,* ***MDM4***
MAPK signaling pathway(K)	0.0248	<0.001	<0.001	*RPS6KA5, TGFBR2, EREG, MET, RAP1B, RAP1A, IGF1*
EGFR tyrosine kinase inhibitor resistance(K)	0.0067	<0.001	<0.001	***PTEN****, PIK3CA, MET, IGF1*

In bold, the genes that were enriched together in the same biological pathway are highlighted. N = National Center for Biotechnology Information (NCBI); R= Reactome; B= BioCarta. FDR= False Discovery Rate.

demonstrated that *PTEN* and *MDM4* expression was significantly downregulated in breast cancer samples compared to non-tumor samples (Fig. 3C and D; FC > 2 and P < 0.05), whereas *TP53* expression was significantly upregulated in breast cancer samples compared to non-tumor samples (Fig. 3E; FC > 2 and P < 0.05).

3.5. miR-19a-3p and miR-130b-3pmay regulate the p53 signaling pathway

Considering that recurrence patients had higher EV-miR-19a-3p and EV-miR-130b-3p levels, and *PTEN* and *MDM4* (predicted targets of miR-19a-3p and has-miR-130b-3p) are related to p53, we next verified whether EV-p53 expression would be varied among

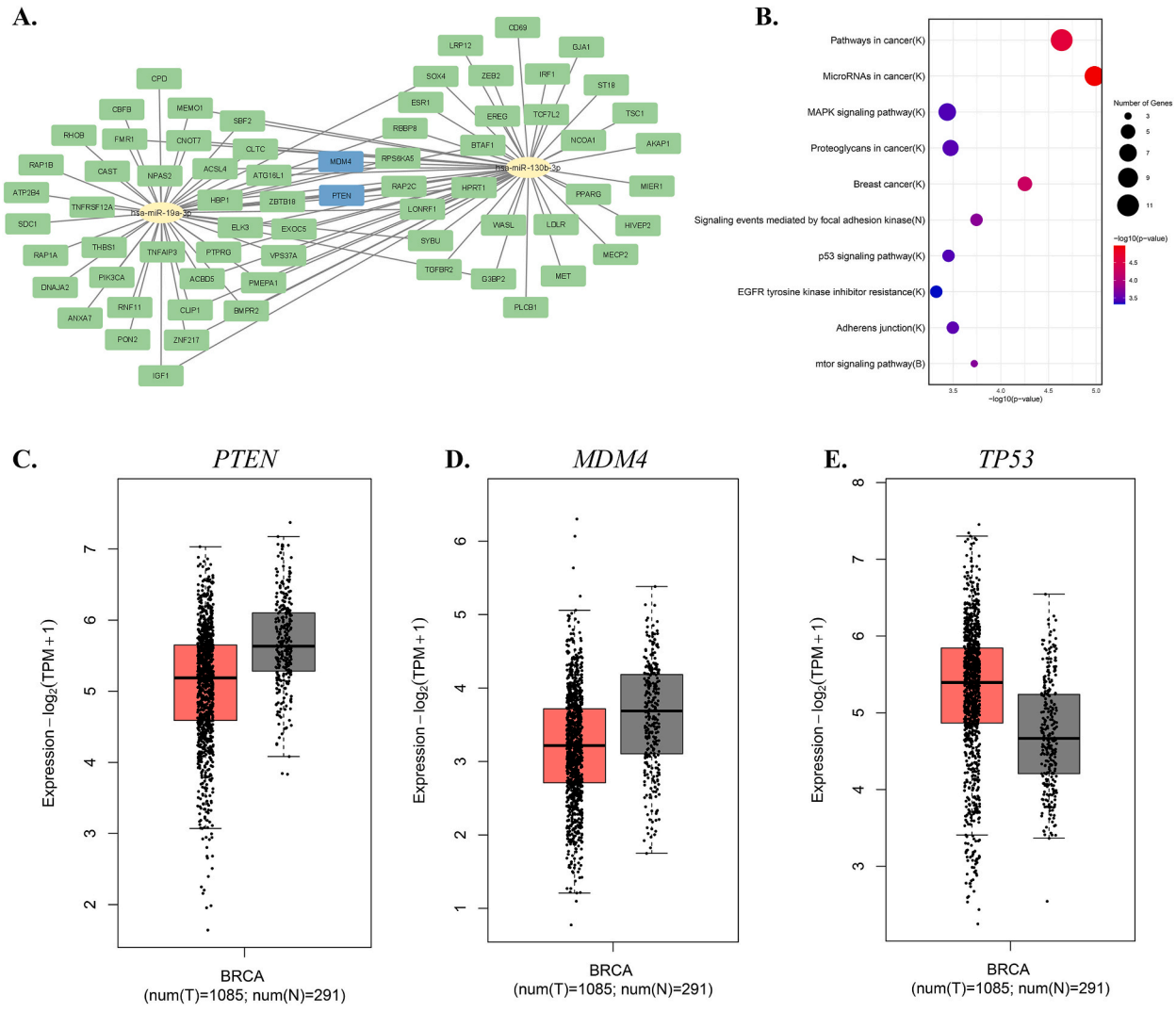

Fig. 3. Pathway enrichment analysis for miR-19a-3p and miR-130b-3p with genes associated with Breast Cancer (BC) recurrence. (A) miRNA-RNAm interaction network predicted to miR-19a-3p and miR-130b-3p described for BC, according to the Cancer Gene Index Annotations (provided by the National Cancer Institute, NCI) using the REACTOME plugin. (B) Dotplot of enrichment pathway result to miR-19a-3p and miR-130b-3p associated with BC recurrence using http://www.bioinformatics.com.cn/. (C) GEPIA 2 database analysis revealed low expression in *PTEN* breast cancer tissues (BRCA). (D) GEPIA 2 database analysis revealed low expression in *MDM4* breast cancer tissues (BRCA). (E) GEPIA 2 database analysis revealed high expression in *TP53* breast cancer tissues (BRCA). K= Kegg pathways; R= Reactome; B= BioCarta. In the boxplots, the red boxes indicate breast cancer tissue samples, while the gray boxes indicate normal samples. (For interpretation of the references to colour in this figure legend, the reader is referred to the Web version of this article.)

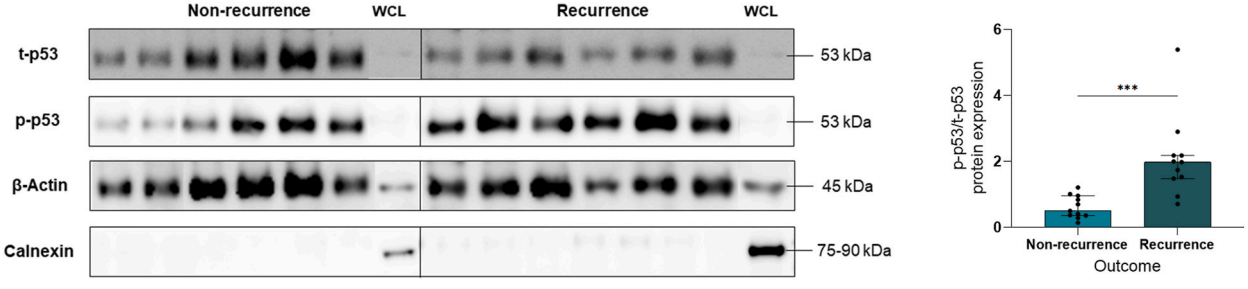

Fig. 4. Western blot analysis for t-p53 and p-p53 in the EVs isolated from both groups (recurrence and non-recurrence patients). The relative p-p53/t-p53 expression is shown as median ± interquartile. ****$p < 0.0001$. WCL: whole cell lysate.

the two groups. For that, we investigated both total (t-p53) and phosphorylated p53 (p-p53) expression by western blotting (Fig. 4). We found that EVs isolated from the recurrence group exhibited a significantly higher expression of p-p53/t-p53, compared to the non-recurrence group ($p < 0.0001$) (Fig. 4 and S2).

3.6. microRNAs and target genes predicted in silico as a prognostic factor in breast cancer

Then, we evaluated the overall survival (OS) and recurrence-free survival (RFS) of the two groups and interrogated whether miR-19a-3p and miR-130b-3p expression levels could influence the OS (Fig. 5). We did not identify significant differences when comparing expression levels of both miRNAs, in OS and RFS of patients with BC (Fig. 5A–D). Kaplan-Meier curve analysis was also performed using the Breast Cancer Gene Expression Profiles (METABRIC) dataset to evaluate OS according to the expression of miR-19a-3p and miR-130b-3p. We verified that miR-19a-3p did not demonstrate significant differences in the OS (Fig. 5 E). Moreover, we investigated that the lowest expression of miR-130b-3p showed an OS = 203,31 months, while the group with the highest expression had an OS = 172,69 months (Fig. 5 F).

Furthermore, we evaluated the OS and RFS of the possible predicted target genes of miR-19a-3p and miR-130b-3p, namely, *PTEN*,

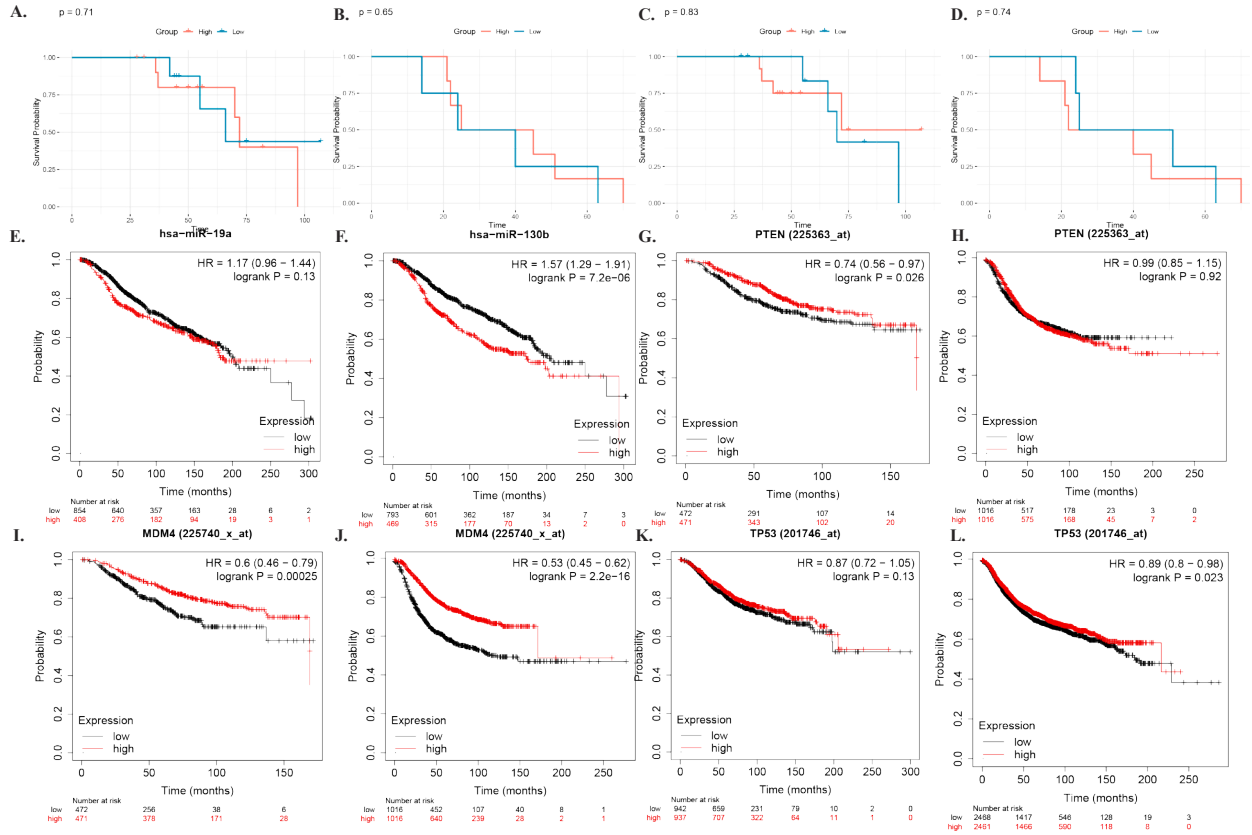

Fig. 5. Prognostic evaluation of miR-19a-3p, miR-130b-3p, PTEN, MDM4, and TP53 in breast cancer patients. (A) Kaplan-Meier curve analysis of overall survival (OS) in breast cancer patients with high and low expression of EV-miR-19a-3p. (B) Kaplan-Meier curve analysis of relapse-free survival (RFS) in breast cancer patients with high and low expression of EV-miR-19a-3p. (C) Kaplan-Meier curve analysis of OS in breast cancer patients with high and low expression of EV-miR-130b-3p. (D) Kaplan-Meier curve analysis of RFS in breast cancer patients with high and low expression of EV-miR-130b-3p. (E) Analysis of the association between miR-19a-3p expression and OS in breast cancer patients using the Kaplan-Meier plotter database. Log-rank test: n = 1262; P = 0.120 (METABRIC dataset). (F) Analysis of the association between miR-130b-3p expression and OS in breast cancer patients using the Kaplan-Meier plotter database. Log-rank test: n = 1262; P < 0.0001 (METABRIC dataset). (G) Analysis of the association between *PTEN* expression and OS in breast cancer patients using the Kaplan-Meier plotter database. Log-rank test: n = 1880; P = 0.026 (225363_at dataset). (H) Analysis of the association between *PTEN* expression and RFS in breast cancer patients using the Kaplan-Meier plotter database. Log-rank test: n = 4934; P = 0.092 (225363_at dataset). (I) Analysis of the association between *MDM4* expression and OS in breast cancer patients using the Kaplan-Meier plotter database. Log-rank test: n = 1880; P < 0.0001 (225740_x_at dataset). (J) Analysis of the association between *MDM4* expression and RFS in breast cancer patients using the Kaplan-Meier plotter database. Log-rank test: n = 4934; P < 0.0001 (225740_x_at dataset). (K) Analysis of the association between *TP53* expression and OS in breast cancer patients using the Kaplan-Meier plotter database. Log-rank test: n = 1880; P = 0.130 (201746_at_x_at dataset). (L) Analysis of the association between *TP53* expression and RFS in breast cancer patients using the Kaplan-Meier plotter database. Log-rank test: n = 4934; P = 0.023 (201746_at dataset). P values for the Log-rank analysis are provided in the figure.

MDM4, and *TP53*. The association between *PTEN, MDM4,* and *TP53* genes with the patient's OS was analyzed using the Kaplan-Meier plotter database (https://kmplot.com/analysis/). Based on the median expression of *PTEN*, *MDM4* and *TP53*, patients were divided into high- and low-expression groups. OS time of patients with high expression of these three genes was significantly longer than patients with low expression of them (Fig. 5G–L). The group with the lowest expression of the *PTEN* gene showed an OS= 68,4 months and RFS= 36 months, while the group with the highest expression had an OS= 106,8 months and RFS= 40,44 months (Fig. 5G and H). For *MDM4* gene we verified that the group with the lowest expression showed an OS= 62,07 months and RFS= 115 months, while the group with the highest expression had an OS= 121 months and RFS= 171,43 months (Fig. 5I and J). Concerning the *TP53* gene, we verified that the group with the lowest expression showed an OS= 84 months and RFS= 185 months, while the group with the highest expression had an OS= 108 months and RFS= 216,66 months (Fig. 5K and L).

4. Discussion

Circulating miRNAs biomarkers for the diagnosis, prognosis, monitoring, and prediction of therapy response in BC through liquid biopsies have been the subject of extensively investigation over the years [27,34–37]. New studies have focused on analyzing EV-miRNAs as potential biomarkers for BC [38]. In the present study, we showed that a higher EV concentration in patients' circulation was associated with patient recurrence. Furthermore, we identified thirty-two EV-miRNAs differentially expressed between the groups, two of which were previously described as having altered expression in breast cancer patients, namely miR-19a-3p and miR-130b-3p being associated with disease recurrence.

MiR-19a-3p, a member of the miR-17-92 cluster, is frequently dysregulated and associated with proliferation, apoptosis, metastasis, and chemoresistance in various cancers [39], including breast cancer [40]. MiR-130b-3p is a key post-transcriptional regulator involved in the progression of several types of cancer, including breast cancer [41]. Yan et al. demonstrated that miR-130b-3p was a negative regulator of the *PTEN* gene. Furthermore, miR-130b-3p promoted angiogenesis in vascular cells through increased proliferation and migration. Our findings corroborate previous studies showing that miR-19a-3p and miR-130b-3p negatively regulate the PTEN gene [39,42]. Jiang et al. found that miR-19a-3p promotes hepatocellular carcinoma metastasis and chemoresistance through repression of PTEN and reduction of its downstream effects on Akt phosphorylation [39]. Meanwhile, exosomes derived from oral squamous cell carcinoma delivered miR-130b-3p to human umbilical vein endothelial cells to promote angiogenesis; these effects were also observed in *in vivo* experiments [42].

At the moment, there are no studies that demonstrate the functional role of the interaction of the miRNAs, miR-19a-3p, and miR-130b-3p with the *MDM4* and *PTEN* genes. However, mechanistic analyses by Egawa et al. indicated that the miR-130 family (miR-130b, miR-301a, and miR-301b) directly target the phosphatase and tensin homolog deleted from chromosome 10 (PTEN), resulting in the upregulation of FAK and Akt phosphorylation in bladder cancer. In summary, the miR-130 family has been seen to play a crucial role in the malignant progression of bladder cancer, and therefore the miR-130 family may be a promising therapeutic target for invasive bladder cancer [43]. Several studies have shown that miR-19a-3p can regulate the expression of *PTEN* and *MDM4* in different tumor types. Lee et al. demonstrated that miR-19a-3p was identified as a mediator of the inhibitory effect on cell proliferation in MCF-7 breast cancer cells. In addition, we saw that overexpression of miR-19a in MCF-7 increased cell proliferation and that target genes of miR-19a-3p, such as *ABCA1* and *PTEN*, were suppressed by overexpression of miR-19a3p [44].

We further showed by *in silico* analysis that the *PTEN* and *MDM4* genes were the only predicted targets for miR-19a-3p and miR-130b-3p associated with breast carcinoma. Among the enriched pathways for *MDM4*, p53 pathways were identified in two different databases. These findings are in line with Francoz et al. study [45], who demonstrated that the MDM4 protein contributes to p53 inhibition and suppresses its transcriptional activity. Moreover, a recent study has shown that *MDM4* binds MDM2 to inhibit p53 activity, and also reported that high p53 expression could be caused by an MDM4 downregulation, resulting in a less efficient MDM2/MDM4 complex [37]. Therefore, we can hypothesize that our results of higher EV-miR-19a-3p, EV-miR-130b-3p, mediated inhibition of *MDM4*, led to p53 overexpression expression.

Our study identified that patients with recurrence disease showed high levels of phosphorylated p53 expression. Previous studies have shown that p53 overexpression leads to a poor response to chemotherapy [46,47]. In a review study published by Yadav et al. it was reported a significant overexpression of p53 in patients with triple-negative BC [48] and its activation is associated with the aggressive form of BC and significantly decreases disease-free survival and overall survival in patients with these tumors [49]. Additional studies have found that p53 overexpression was associated with the mutation of this protein. Thus, the authors suggested that despite the overexpression of p53 that has been observed in BC patients, the deficiency in the function of this protein caused by the mutation may result in loss of cell cycle control (lack of G1 arrest) and possibly allow tumor cells to enter the phase more effectively of mitosis, thereby supporting the cytotoxicity of chemotherapy [47]. Post-translational modifications, such as phosphorylation at specific serine residues, activate the protein to bind DNA and transactivate downstream 'effector' genes responsible for mediating the p53 tumor-suppressive actions [50]. Phosphorylation results in an increase in active p53 protein levels due to reduced proteolytic degradation dependent on the MDM2 and MDM4 family of proteins, and increased affinity of p53 for DNA [51]. Hence, Toledo et al. suggested that MDM4 could also be an exciting target in anticancer strategies [52]. Direct evidence of this was obtained with the mouse mutant p53 lacking the proline-rich domain (p53DeltaP) when its ability to suppress oncogene-induced tumors was analyzed in several genetic contexts according to the regulation of MDM2 and MDM4 [52]. Therefore, our findings corroborate with the identified in the literature. However, additional studies need to be conducted to investigate the effect that leads patients with recurrent BC to present an elevated expression of phosphorylated p53.

We investigated the potential association between the concentration of EV-miR-19a-3p and EV-miR-130b-3p and their prognostic value in BC patients. However, our data did significant differences. Consequently, further studies involving a larger cohort of patients

are necessary to elucidate the potential prognostic value of these EV-miRNAs. Nevertheless, in our analyses utilizing the publicly available METABRIC dataset, we observed that elevated levels of miR-130b-3p expression were associated with worse OS. Additionally, *in silico* analysis indicated that low expression of the *PTEN* and *MDM4* genes, which were predicted targets of regulation for EV-miR-19a-3p and EV-miR-130b-3p, was correlated with poorer OS and RFS in BC patients. These findings suggest that the dysregulation of EV-miR-130b-3p and the downstream target genes *PTEN* and *MDM4* may have implications for the prognosis of BC patients. However, further experimental and clinical investigations are warranted to validate these associations and establish their clinical significance.

In summary, our findings suggest that EV-miR-19a-3p and EV-miR-130b-3p play a role in the post-transcriptionally regulation of the PTEN and MDM4 genes. This dysregulation leads to decreased expression of *PTEN* and *MDM4* in patients with recurrent BC. As a result, *MDM4* cannot effectively regulate the p53 signaling pathway, leading to p53 overexpression (Fig. 6).

Despite the novelty of our findings, this study has some limitations. The first issue is the limited number of samples analyzed. However, we performed a large-scale technique, nCounter (NanoString Technologies), a robust, accurate, and precise approach for evaluating miRNAs expression profile. Second is the absence of EVs evaluation by transmission electron microscopy, and the possible presence of lipoproteins that are co-isolated with the EVs that are not removed by ultracentrifugation. However, this study evaluated three different EV markers by WB and characterized the EVs by NTA. It is important to highlight that further studies are warranted to confirm whether *PTEN* and *MDM4* genes were potential targets of miR-19a-3p and miR-130b-3p, causing the dysregulation of the p53 signaling pathway in BC. Finally, it is necessary that the expression of EV-miR-19a-3p and EV-miR-130b-3p be validated in a larger cohort for confirmation as biomarkers of breast cancer recurrence.

5. Conclusion

In conclusion, the results of the present study revealed that the BC recurrence samples showed a greater concentration of EVs. In the miRNA profile of EVs, we found higher EV-miR-19a-3p and EV-miR-130b-3p expression in patients with BC recurrence, which was associated with a poor prognosis. *MDM4* and *PTEN* proteins were identified as potential targets of EV-miR-19a-3p and EV-miR-130b-3p, leading to alteration of the p53 pathway in BC.

Data availability statement

The datasets generated and analyzed in this study can be found in the Gene Expression Omnibus (GEO) repository [https://www.ncbi.nlm.nih.gov/geo/], accession GSE236845.

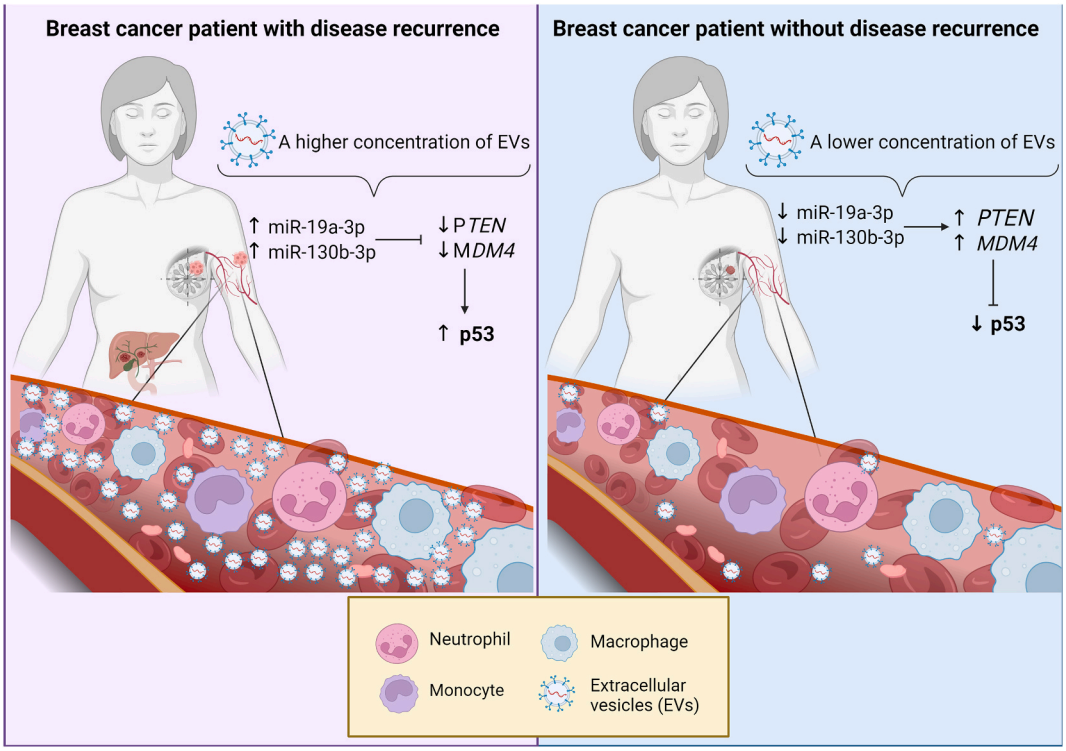

Fig. 6. Graphic summary on the regulation of EV-miR-19a-3p and EV-miR-130b-3p expression in recurrent and non-recurrent breast cancer.

Ethics statement

The study followed ethical standards set by the institutional research committee and complied with the 1964 Declaration of Helsinki and its later amendments. The research project was approved by the Research Ethics Committee of Fundação Pio XII – Barretos Cancer Hospital (CEP-HCB), following Resolution CNS 466/2012 and Operational Standard nº 001/2013 of CNS and was registered at CEP-HCB under Protocol nº 1428/2017. All identifying information about the study participants was securely encrypted in the database to protect the confidentiality of the data and ensure participant anonymity. The research participants provided their written informed consent to participate in this study.

Funding

This research was funded by São Paulo Research Foundation (FAPESP) (grant #2018/19476–9 and grant #2018/17133–7), the Research Incentive Program of Barretos Cancer Hospital (PAIP) and by the Public Ministry of Labor Campinas (Research, Prevention, and Education of Occupational Cancer).

CRediT authorship contribution statement

Rhafaela Lima Causin: Writing – review & editing, Writing – original draft, Visualization, Methodology, Investigation, Formal analysis, Data curation, Conceptualization. **Mariana Regatieri Polezi:** Methodology, Conceptualization. **Ana Julia Aguiar de Freitas:** Writing – review & editing, Methodology, Formal analysis. **Stéphanie Calfa:** Writing – review & editing, Methodology, Formal analysis. **Wanessa Fernanda Altei:** Writing – review & editing, Methodology, Formal analysis. **Júlia Oliveira Dias:** Writing – review & editing, Methodology, Formal analysis. **Ana Carolina Laus:** Writing – review & editing, Methodology. **Danielle Pessôa-Pereira:** Writing – review & editing, Methodology. **Tatiana Takahasi Komoto:** Writing – review & editing. **Adriane Feijó Evangelista:** Writing – review & editing, Methodology, Formal analysis. **Cristiano de Pádua Souza:** Formal analysis, Methodology, Writing – review & editing. **Rui Manuel Reis:** Writing – review & editing, Resources, Methodology, Investigation, Funding acquisition, Formal analysis, Conceptualization. **Marcia Maria Chiquitelli Marques:** Conceptualization, Formal analysis, Funding acquisition, Investigation, Methodology, Project administration, Supervision, Writing – review & editing.

Declaration of competing interest

The authors declare that they have no known competing financial interests or personal relationships that could have appeared to influence the work reported in this paper.

Acknowledgments

The authors would like to thank all the women who participated in the study, the Office of Projects and Technological Innovation of Barretos Cancer Hospital, and pathologists from the Department of Pathology to the Center for the Epidemiology and Biostatistics of Barretos Cancer Hospital (especially Marco Antônio Oliveira). This research was funded by the Research Incentive Program of Barretos Cancer Hospital (PAIP) and by the Public Ministry of Labor Campinas (Research, Prevention, and Education of Occupational Cancer). The authors are grateful to the researchers André van Helvoort Lengert for the technical-scientific support in the characterization of EVs and Dr. Juliana Monte Real for helping and teaching the use of the NanoSight equipment.

Appendix A. Supplementary data

Supplementary data to this article can be found online at https://doi.org/10.1016/j.heliyon.2024.e33933.

References

[1] IARC, Fact sheets by cancer [internet], Available from: https://gco.iarc.fr/today/data/factsheets/cancers/20-Breast-fact-sheet.pdf, 2020.
[2] H. Sung, J. Ferlay, R.L. Siegel, M. Laversanne, I. Soerjomataram, A. Jemal, et al., Global cancer statistics 2020: GLOBOCAN estimates of incidence and mortality worldwide for 36 cancers in 185 countries, Ca - Cancer J. Clin. (2021).
[3] C.M. Perou, T. Sørlie, M.B. Eisen, M. van de Rijn, S.S. Jeffrey, C.A. Rees, et al., Molecular Portraits of Human Breast Tumours. Nature, 406, Nature Publishing Group, 2000, pp. 747–752.
[4] D.C. Koboldt, R.S. Fulton, M.D. McLellan, H. Schmidt, J. Kalicki-Veizer, J.F. McMichael, et al., Comprehensive Molecular Portraits of Human Breast Tumours. Nature, 490, Nature Publishing Group, 2012, pp. 61–70.
[5] Y. Lee, J. Ni, J. Beretov, V.C. Wasinger, P. Graham, Y. Li, Recent advances of small extracellular vesicle biomarkers in breast cancer diagnosis and prognosis, Mol. Cancer 22 (2023) 33.
[6] S. Koren, M. Bentires-Alj, Breast tumor heterogeneity: source of fitness, hurdle for therapy, Mol. Cell 60 (2015) 537–546.
[7] R. Clarke, J.J. Tyson, J.M. Dixon, Endocrine resistance in breast cancer – an overview and update, Mol. Cell. Endocrinol. 418 (2015) 220–234.
[8] J. Liu, Y. Chen, F. Pei, C. Zeng, Y. Yao, W. Liao, et al., Extracellular vesicles in liquid biopsies: potential for disease diagnosis, BioMed Res. Int. 2021 (2021) 6611244.

[9] H. Valadi, K. Ekström, A. Bossios, M. Sjöstrand, J.J. Lee, J.O. Lötvall, Exosome-mediated Transfer of mRNAs and microRNAs Is a Novel Mechanism of Genetic Exchange between Cells. Nat Cell Biol, 9, Nature Publishing Group, 2007, pp. 654–659.
[10] G. van Niel, G. D'Angelo, G. Raposo, Shedding light on the cell biology of extracellular vesicles, Nat. Rev. Mol. Cell Biol. 19 (2018) 213–228.
[11] C. Théry, K.W. Witwer, E. Aikawa, M.J. Alcaraz, J.D. Anderson, R. Andriantsitohaina, et al., Minimal information for studies of extracellular vesicles 2018 (MISEV2018): a position statement of the International Society for Extracellular Vesicles and update of the MISEV2014 guidelines, J. Extracell. Vesicles 7 (2018) 1535750.
[12] Z. Weng, B. Zhang, C. Wu, F. Yu, B. Han, B. Li, et al., Therapeutic roles of mesenchymal stem cell-derived extracellular vesicles in cancer, J. Hematol. Oncol. 14 (2021) 136.
[13] H.-X. Wang, O. Gires, Tumor-derived extracellular vesicles in breast cancer: from bench to bedside, Cancer Lett. 460 (2019) 54–64.
[14] M. Ha, V.N. Kim, Regulation of microRNA Biogenesis. Nat Rev Mol Cell Biol, 15, Nature Publishing Group, 2014, pp. 509–524.
[15] M.I. Almeida, R.M. Reis, G.A. Calin, MicroRNA history: discovery, recent applications, and next frontiers, Mutat. Res. 717 (2011) 1–8.
[16] R. Garzon, G. Marcucci, C.M. Croce, Targeting microRNAs in cancer: rationale, strategies and challenges, Nat. Rev. Drug Discov. 9 (2010) 775–789.
[17] A.F. Evangelista, R.J. Oliveira, V.A. O Silva, R.A. D C Vieira, R.M. Reis, M.M. C Marques, Integrated analysis of mRNA and miRNA profiles revealed the role of miR-193 and miR-210 as potential regulatory biomarkers in different molecular subtypes of breast cancer, BMC Cancer 21 (2021) 76.
[18] D. Pessôa-Pereira, A.F. Evangelista, R.L. Causin, R.A. da Costa Vieira, L.F. Abrahão-Machado, I.V.V. Santana, et al., miRNA expression profiling of hereditary breast tumors from BRCA1- and BRCA2-germline mutation carriers in Brazil, BMC Cancer 20 (2020) 143.
[19] A.L.R. Bordinhão, A.F. Evangelista, R.J.S. Oliveira, T. Macedo, H.C. Silveira, R.M. Reis, et al., MicroRNA profiling in human breast cancer cell lines exposed to the anti-neoplastic drug cediranib, Oncol. Rep. 36 (2016) 3197–3206.
[20] M. Selbach, B. Schwanhäusser, N. Thierfelder, Z. Fang, R. Khanin, N. Rajewsky, Widespread changes in protein synthesis induced by microRNAs, Nature 455 (2008) 58–63.
[21] S. Uhlmann, H. Mannsperger, J.D. Zhang, E.-Á. Horvat, C. Schmidt, M. Küblbeck, et al., Global microRNA level regulation of EGFR-driven cell-cycle protein network in breast cancer, Mol. Syst. Biol. 8 (2012) 570.
[22] B.N. Hannafon, Y.D. Trigoso, C.L. Calloway, Y.D. Zhao, D.H. Lum, A.L. Welm, et al., Plasma exosome microRNAs are indicative of breast cancer, Breast Cancer Res. 18 (2016) 90.
[23] A. Sueta, Y. Yamamoto, M. Tomiguchi, T. Takeshita, M. Yamamoto-Ibusuki, H. Iwase, Differential expression of exosomal miRNAs between breast cancer patients with and without recurrence, Oncotarget 8 (2017) 69934–69944.
[24] A.C. Neuber, C.H. Tostes, A.G. Ribeiro, G.T. Marczynski, T.T. Komoto, C.D. Rogeri, et al., The biobank of barretos cancer hospital: 14 years of experience in cancer research, Cell Tissue Bank. 23 (2022) 271–284.
[25] P.A. Harris, R. Taylor, R. Thielke, J. Payne, N. Gonzalez, J.G. Conde, Research Electronic Data Capture (REDCap) - a metadata-driven methodology and workflow process for providing translational research informatics support, J. Biomed. Inf. 42 (2009) 377–381.
[26] NanoString Technologies, nCounter® Human V3 miRNA Expression Assay, 2015.
[27] K.C.B. Souza, A.F. Evangelista, L.F. Leal, C.P. Souza, R.A. Vieira, R.L. Causin, et al., Identification of cell-free circulating MicroRNAs for the detection of early breast cancer and molecular subtyping, JAMA Oncol. 2019 (2019) 8393769.
[28] T. Tokar, C. Pastrello, A.E.M. Rossos, M. Abovsky, A.-C. Hauschild, M. Tsay, et al., mirDIP 4.1—integrative database of human microRNA target predictions, Nucleic Acids Res. 46 (2018) D360–D370.
[29] E.A. Shirdel, W. Xie, T.W. Mak, I. Jurisica, NAViGaTing the micronome–using multiple microRNA prediction databases to identify signalling pathway-associated microRNAs, PLoS One 6 (2011) e17429.
[30] Z. Tang, B. Kang, C. Li, T. Chen, Z. Zhang, GEPIA2: an enhanced web server for large-scale expression profiling and interactive analysis, Nucleic Acids Res. 47 (2019) W556–W560.
[31] A. Lánczky, Á. Nagy, G. Bottai, G. Munkácsy, A. Szabó, L. Santarpia, et al., miRpower: a web-tool to validate survival-associated miRNAs utilizing expression data from 2178 breast cancer patients, Breast Cancer Res. Treat. 160 (2016) 439–446.
[32] The Cancer Gene Index Gene-Disease and Gene-Compound XML Documents - ICR - Cancer Gene Index - NCI Wiki [Internet]. [cited 2023 Aug 2]. Available from: https://wiki.nci.nih.gov/display/cageneindex/The+Cancer+Gene+Index+Gene-Disease+and+Gene-Compound+XML+Documents.
[33] P. Shannon, A. Markiel, O. Ozier, N.S. Baliga, J.T. Wang, D. Ramage, et al., Cytoscape: a software environment for integrated models of biomolecular interaction networks, Genome Res. 13 (2003) 2498–2504.
[34] R. Hamam, D. Hamam, K.A. Alsaleh, M. Kassem, W. Zaher, M. Alfayez, et al., Circulating microRNAs in breast cancer: novel diagnostic and prognostic biomarkers, Cell Death Dis. 8 (2017) e3045.
[35] J. Gao, Q. Zhang, J. Xu, L. Guo, X. Li, Clinical significance of serum miR-21 in breast cancer compared with CA153 and CEA, Chin. J. Cancer Res. 25 (2013) 743–748.
[36] M.G. Schrauder, R. Strick, R. Schulz-Wendtland, P.L. Strissel, L. Kahmann, C.R. Loehberg, et al., Circulating micro-RNAs as potential blood-based markers for early stage breast cancer detection, PLOS ONE. Public Library of Science 7 (2012) e29770.
[37] AJA de Freitas, R.L. Causin, M.B. Varuzza, S. Calfa, C.M.T. Hidalgo Filho, T.T. Komoto, et al., Liquid biopsy as a tool for the diagnosis, treatment, and monitoring of breast cancer, Int. J. Mol. Sci. 23 (2022) 9952.
[38] P.M.M. Ozawa, E. Vieira, D.S. Lemos, I.L.M. Souza, S.M. Zanata, V.C. Pankievicz, et al., Identification of miRNAs enriched in extracellular vesicles derived from serum samples of breast cancer patients, Biomolecules 10 (2020) 150.
[39] X.-M. Jiang, X.-N. Yu, T.-T. Liu, H.-R. Zhu, X. Shi, E. Bilegsaikhan, et al., microRNA-19a-3p promotes tumor metastasis and chemoresistance through the PTEN/Akt pathway in hepatocellular carcinoma, Biomed. Pharmacother. 105 (2018) 1147–1154.
[40] X. Li, W. Xie, C. Xie, C. Huang, J. Zhu, Z. Liang, et al., Curcumin modulates miR-19/PTEN/AKT/p53 axis to suppress bisphenol A-induced MCF-7 breast cancer cell proliferation, Phytother Res. 28 (2014) 1553–1560.
[41] Y. Shui, X. Yu, R. Duan, Q. Bao, J. Wu, H. Yuan, et al., miR-130b-3p inhibits cell invasion and migration by targeting the Notch ligand Delta-like 1 in breast carcinoma, Gene 609 (2017) 80–87.
[42] W. Yan, Y. Wang, Y. Chen, Y. Guo, Q. Li, X. Wei, Exosomal miR-130b-3p promotes progression and tubular formation through targeting PTEN in oral squamous cell carcinoma [cited 2023 Jun 30], Frontiers in Cell and Developmental Biology [Internet] 9 (2021). Available from: https://www.frontiersin.org/articles/10.3389/fcell.2021.616306.
[43] H. Egawa, K. Jingushi, T. Hirono, Y. Ueda, K. Kitae, W. Nakata, et al., The miR-130 family promotes cell migration and invasion in bladder cancer through FAK and Akt phosphorylation by regulating PTEN, Sci. Rep. 6 (2016) 20574.
[44] S. Lee, H. Lee, H. Bae, E.H. Choi, S.J. Kim, Epigenetic silencing of miR-19a-3p by cold atmospheric plasma contributes to proliferation inhibition of the MCF-7 breast cancer cell, Sci. Rep. 6 (2016) 30005.
[45] S. Francoz, P. Froment, S. Bogaerts, S. De Clercq, M. Maetens, G. Doumont, et al., Mdm4 and Mdm2 cooperate to inhibit p53 activity in proliferating and quiescent cells in vivo, Proc. Natl. Acad. Sci. U. S. A. 103 (2006) 3232–3237.
[46] T. Hasebe, N. Tamura, N. Okada, T. Hojo, S. Akashi-Tanaka, C. Shimizu, et al., p53 expression in tumor-stromal fibroblasts is closely associated with the nodal metastasis and outcome of patients with invasive ductal carcinoma who received neoadjuvant therapy, Hum. Pathol. 41 (2010) 262–270.
[47] D. Kandioler-Eckersberger, C. Ludwig, M. Rudas, S. Kappel, E. Janschek, C. Wenzel, et al., TP53 mutation and p53 overexpression for prediction of response to neoadjuvant treatment in breast cancer patients, Clin. Cancer Res. 6 (2000) 50–56.
[48] B.S. Yadav, P. Chanana, S. Jhamb, Biomarkers in triple negative breast cancer: a review, World J. Clin. Oncol. 6 (2015) 252–263.
[49] K.A. Dookeran, J.J. Dignam, K. Ferrer, M. Sekosan, W. McCaskill-Stevens, S. Gehlert, p53 as a marker of prognosis in African-American women with breast cancer, Ann. Surg Oncol. 17 (2010) 1398–1405.

[50] M. Gasco, S. Shami, T. Crook, The p53 pathway in breast cancer, Breast Cancer Res. 4 (2002) 70.
[51] F. Toledo, G.M. Wahl, MDM2 and MDM4: p53 regulators as targets in anticancer therapy, Int. J. Biochem. Cell Biol. 39 (2007) 1476–1482.
[52] F. Toledo, K.A. Krummel, C.J. Lee, C.-W. Liu, L.-W. Rodewald, M. Tang, et al., A mouse p53 mutant lacking the proline-rich domain rescues Mdm4 deficiency and provides insight into the Mdm2-Mdm4-p53 regulatory network, Cancer Cell 9 (2006) 273–285.